The ROCK-Ezrin Signaling Pathway Mediates LPS-Induced Cytokine Production in A549 Cells

Ning Ding (dingninggz@hotmail.com)
Shandong University Cheeloo College of Medicine https://orcid.org/0000-0003-0087-4077
Huiqing Li
Shandong University Cheeloo College of Medicine
Baofeng Gao
Shandong University Cheeloo College of Medicine
Yunlong Lei
Shandong University Cheeloo College of Medicine
Zengzhen Zhang
Shandong University Cheeloo College of Medicine

Research article

Keywords: ROCK, ezrin, LPS, signal pathway, inflammation

Posted Date: August 30th, 2021

DOI: https://doi.org/10.21203/rs.3.rs-786438/v1

Abstract

Background: Ezrin/radixin/moesin proteins (ERMs) are members of the protein 4.1 superfamily and function as linkers that connect the actin cytoskeleton to the plasma membrane of cells. ERMs also play critical role in the Lipopolysaccharide (LPS)-induced inflammatory response. However, the signaling mechanisms involved remain unclear. This study aims to investigate the potential role of the rho-associated coiled-coil containing protein kinase (ROCK) pathway in LPS-induced ezrin phosphorylation and cytokine production in A549 cells.

Methods: Cultured A549 cells were treated with LPS. The expression and localization of ezrin in A549 cells were analyzed by Western bloting and immunoflurescence. The activation of RhoA/ROCK was assessed by Western bloting and RhoA activity assays. The interaction of ezrin with Syk and myeloid differentiation factor 88 (MyD88)/IL-1R-associated kinase 1 (IRAK-1) was investigated using co-immunoprecipitation. The activation of nuclear factor-κB (NF-κB) and mitogen-activated protein kinase (MAPK) was measured with electrophoretic mobility shift assay and Western blotting. ELISA and Western bloting were performed to detect tumor necrosis factor-α (TNF-α), interleukin-1β (IL-1β), and high mobility group box 1 protein (HMGB1) release into the culture supernatant and cellular HMGB1 levels.

Results: Here, we show that LPS induced ezrin phosphorylation in a concentration- and time-dependent manner. The blockade of RhoA/ROCK inhibited LPS-induced ezrin phosphorylation and its translocation from the cytoplasm to the cell membrane. Co-immunoprecipitation assays further revealed that ezrin associated with Syk constitutively, but only associated with MyD88/IRAK-1 upon LPS challenge. Moreover, LPS-induced p38 and nuclear NF-κB activation was found to be ezrin dependent. The suppression of ezrin by siRNA or the blockade of ROCK activation with Y-27632 reduced the production of TNF-α, IL-1β, and HMGB1 in response to LPS.

Conclusions: Our findings reveal a novel regulatory mechanism involving ezrin in LPS induced the production of pro-inflammatory cytokines, and highlight the importance of the RhoA/ROCK-MyD88/IRAK1-ezrin/Syk axis. Data presented in this manuscript provide novel insights into the signaling pathways activated in A549 cells by LPS.

Introduction

Acute lung injury (ALI)/acute respiratory distress syndrome (ARDS) is a clinical syndrome that involves persistent lung inflammation caused by various direct and indirect stimuli. The most common risk factor that leads to ALI/ARDS is bacterial sepsis with either a pulmonary or non-pulmonary source [1]. Lipopolysaccharide (LPS), the endotoxin portion of the gram-negative bacteria cell wall, is one of the most potent inducers of inflammatory signaling and has been proven to be an important factor that can lead to ALI/ARDS [2].

It is well known that LPS binds toll-like receptor 4 (TLR4) and stimulates both mitogen-activated protein kinase (MAPK) and nuclear factor-κB (NF-κB) to induce the synthesis and release of inflammatory

cytokines. Ezrin/radixin/moesin proteins (ERMs) are members of the protein 4.1 superfamily and function as linkers that connect the actin cytoskeleton to the plasma membrane of cells [3]. Recent studies have reported that ERM phosphorylation results in the loss of endothelial barrier integrity, thus leading to lung inflammation [4, 5]. Another research involving an LPS-induced ALI model showed that the introduction of a phospho-null moesin mutant into the mouse lung significantly attenuated LPS-induced lung inflammation and vascular leakage, thus suggesting that moesin dephosphorylation protects against lung injury [6]. Studies further highlighted their involvement in the LPS-induced production of inflammatory cytokines. Ezrin is reported to regulate the expression of interleukin-10 (IL-10) in B cells upon LPS stimulation [7] while the moesin silencing with specific siRNA transfection has been shown to lead to a significant reduction of LPS-induced tumor necrosis factor-α (TNF-α), IL-6, IL-18, and IL-1β production in human microvascular endothelial cells [8]. Therefore, it appears that ERMs play a critical role in the LPS- induced inflammatory response. However, the signal transduction mechanisms involved in this process have yet to be elucidated.

Rho-associated coiled-coil containing protein kinase (ROCK), a downstream target effecter of small GTPase RhoA, is known to participate in a range of cell processes, including migration, apoptosis, proliferation, motility, and contraction, that are mediated by reorganization of the actin cytoskeleton [9]. A number of recent studies have linked the RhoA/ROCK signaling pathway to LPS-induced inflammatory diseases, including sepsis and ALI [10–13]. A previous study showed that the inhibition of ROCK activity was able to improve endothelial permeability and alleviate the inflammatory reaction, oxidative stress, and cellular apoptosis, in a sepsisinduced rat model of ALI [14]. ROCK is known to regulate the cross-linking activities of ERMs and mediate phosphorylation of the C-terminal domain of ERM proteins to stabilize their active state [15]. Therefore, we hypothesized that the RhoA/ROCK pathway plays a key role in the activation of ERMs. In the present study, we tested whether ezrin is activated *via* the RhoA/ROCK pathway and investigated potential signal transduction mechanisms involved in the response to LPS. The results derived from this systematic study will not only improve our understanding of the mechanisms associated with the action of ezrin in regulating the inflammatory reaction in airway epithelial cells, but also offers an opportunity to target ezrin when developing novel therapies for the management of ALI/ARDS.

Material And Methods

Cell culture and treatment

A549 cell line was obtained from the American Type Culture Collection (Manassas, VA, USA). A549 cells were grown in Dulbecco's Modified Eagle Medium (DMEM) supplemented with 10% fetal bovine serum and antibiotic/antimycotic. For dose-response experiments, cells were treated with LPS (Sigma, St. Louis, MO, USA) at concentrations of 0.1, 1 and 10 μg/ml for 3 h. For time-course experiments, cells were treated with 10 μg/ml of LPS for 0.5, 1, 3, 6 and 12 h. In ROCK blockade experiments, cells were pretreated with Y-27632 (Sigma, St. Louis, MO, USA) at a concentration of 50 μM for 1 h before being exposed to LPS (10

μg/ml). Cells were seeded in petri dishes at a density of 5×10^4/ml for immunofluorescence and 5×10^5/ml for western blotting and ELISA.

Western blotting

After treatment, cells were washed with ice-cold phosphate buffered saline (PBS) and then exposed to radio immunoprecipitation assay (RIPA) lysis buffer [supplemented with 1mM phenylmethylsulfonyl fluoride (PMSF) and 1mM protease inhibitor cocktail (PIC)]. A bicinchoninic acid (BCA) protein analysis kit (Pierce, Rockford, IL, USA) was used to quantify protein concentration. Equal amounts of protein were resolved by sodium dodecyl sulfate polyacrylamide gel electrophoresis (SDS-PAGE) and then transferred to 0.45 μm polyvinyl difluoride (PVDF) membranes. Membranes were then blocked with 5% bovine serum albumin (BSA) diluted in tris-buffered saline containing Tween 20 (TBST) for 1 h and then incubated with primary antibodies against p38, p-p38, ERK1/2, p-ERK1/2, JNK, p-JNK (Cell Signaling, Danvers, MA, USA); and ezrin, p-ezrin, RhoA, ROCK1, IKKβ, p-IKKβ, IκBα, p-IκBα and high mobility group box 1 protein (HMGB1) (Abcam, Cambridge, MA, USA). β-actin was used as internal standard. Following incubation, PVDF membranes were washed with TBST and then incubated with peroxidase-conjugated specific secondary antibody for 1 h at room temperature. Bands were visualized by chemiluminescence, representative images were acquired, and Image J software (NIH Image, Bethesda, MD, USA) was used to quantify the density of each band.

RhoA activity assays

Active GTP-bound RhoA was detected using lysates collected from A549 cells subjected to pull-down assay with a RhoA activation assay kit (Abcam, Cambridge, MA, USA); this kit was used in accordance with the manufacturer's indications. In brief, supernatants were incubated with anti-active RhoA monoclonal antibody and a protein A/G agarose bead slurry on a rotator. Bead-precipitated proteins were then fractionated and immunoblotted with an antibody against RhoA (Abcam, Cambridge, MA, USA).

Co-immunoprecipitation

Whole cell lysates were incubated overnight with anti-ezrin antibody. Immune complexes were precipitated with protein A/G agarose beads for 6 h and then washed three times with immunoprecipitation buffer. Immunoprecipitated proteins were then eluted with 2 × SDS loading buffer and analyzed by western blotting using anti-Syk, anti-myeloid differentiation factor 88 (MyD88), anti-IL-1R-associated kinase 1 (IRAK-1), or anti-ezrin (Abcam, Cambridge, MA, USA), as described above.

Fluorescence microscopy

Cells were washed with PBS and fixed with 4% paraformaldehyde for 30 min at room temperature. Cells were then permeabilized with 0.5% Triton X-100 for 10 min and blocked with 5% BSA in TBST for 1 h. The samples were then incubated with anti-p-ezrin antibody (Abcam, Cambridge, MA, USA) in TBST overnight at 4°C. The next morning, the cells were washed with TBST and then incubated with Alexa Fluor 488-conjugated AffiniPure goat anti-rabbit IgG (ZSGB-BIO, Beijing, China) and Rhodamine-phalloidin (Molecular Probes, Carlsbad, CA, USA) to stain p-ezrin and F-actin, respectively. Nuclei were stained with

DAPI (Invitrogen, Carlsbad, CA, USA). Samples were washed three times with TBST prior to confocal microscopy (Olympus FV1000, Olympus Corp., Tokyo, Japan).

siRNA transfection

For transient knockdown experiments, A549 cells were transfected with ezrin- specific siRNA (ezrin-siRNA) or control siRNA (Santa Cruz Biotechnology, Santa Cruz, CA, USA). Cells were first plated onto 6-well plates. Ezrin siRNA or control siRNA duplexes were diluted to a final concentration of 10 μM in OptiMem (Invitrogen, San Diego, CA, USA) and incubated with Lipofectamine 2000 transfection reagent (Thermo Fisher Scientific, Waltham, MA, USA) at room temperature for 15 min. The mixture was then incubated with A549 cells in serum for 18 h at 37°C. Cells were then washed twice with sterile PBS and incubated in William's E medium supplemented with 5% calf serum for 24 h prior to exposure to LPS.

Reverse transcription PCR and quantitative real-time PCR

RNA was extracted from A549 cells using the RNeasy Mini Kit (Qiagen, Valencia, CA, USA). An iScript reverse transcription supermix kit (Bio-Rad, Hercules, CA, USA) was used for reverse transcription. PCR amplification mixtures were prepared using iTaq™ Fast SYBR Green Supermix with ROX (Bio-Rad, Hercules, CA, USA). The sequences of the primers for ezrin were as follows: forward 5'-GTGGGATGCTCAAAGATAATGC-3; reverse 5'-CACCTCGATGGTGTCAGGCT-3'. Real-time PCR was performed using an Mx3000p system (Stratagene, La Jolla, CA, USA) and all samples were run in triplicate. The quantification of gene expression levels was calculated relative to β-actin.

Electrophoretic mobility shift assays (EMSAs)

NF-κB DNA-binding activity was measured by EMSA using nuclear extracts prepared from A549 cells. First, cells were scraped into 1 mL of PBS and centrifuged. The pelleted cells were then homogenized in buffer A, incubated on ice for 15 min, and then centrifuged for 5 min. Nuclear proteins were extracted by gently resuspending the nuclei pellet in buffer C along with buffer D (identical to buffer C but contains 1.6 M KCl) added in a dropwise fashion. After 1 h incubation on ice, supernatants were collected by centrifugation at 13,800 ×*g* for 15 min. An NF-κB specific oligonucleotide was end-labeled with [γ-^{32}P] ATP using T4 polynucleotide kinase (New England Biolabs, Ipswich, MA, USA) and purified on a G-50 Sephadex spin column. Nuclear proteins were then incubated with ^{32}P-labeled oligonucleotide for 30 min at room temperature. The DNA protein complexes were then resolved on a 4% non-denaturing polyacrylamide gel and subjected to autoradiography.

CCK-8 assays

According to the manufacturer’s instructions, CCK-8 solution (Dojindo, Tokyo, Japan) was added to each well in a 96-well plate. A549 cells were incubated with Y-27632 (10 μM or 50 μM) for 4 h. Cells were then incubated for another 2 h in a 37°C, 5% CO_2 incubator. We also used a control group (without Y-27632). Finally, the OD values for each well were measured at 450 nm using a microplate reader.

ELISA assays

Samples were centrifuged at 1000 ×*g* at 4°C for 20 min; supernatants were then used to determine the levels of TNF-α, IL-1β, and HMGB1, in accordance with the manufacturer's instructions (Elabscience Biotechnology). All samples were assayed in triplicate.

Statistical Analysis

All statistical analyses were performed using SigmaPlot 11.0 (Systat Software, Point Richmond, CA). Data are expressed as mean ± standard deviation (SD). Normality of sampled data was assessed using the Shapiro-Wilk test. Comparisons of two groups under the same treatment were performed by the Student's *t*-test. One-way analysis of variance (ANOVA) was used for multiple group comparisons. When statistical heterogeneity occurred, Welch's test was used. Significance was established at $p < 0.05$.

Results

LPS induced ezrin phosphorylation in A549 cells

A549 cells were treated with LPS at different concentrations and time intervals. P-ezrin protein level was then evaluated by Western blotting. We found that the fold increases of p-ezrin were 1.22 ± 0.15, 1.46 ± 0.22 and 1.83 ± 0.23 with 0.1μg/ml, 1μg/ml and 10μg/ml of LPS treatment, respectively ($p < 0.05$, Fig. 1A). In the time-course experiment, the upregulation of p-ezrin began at 0.5 h (a fold increase of 1.17 ± 0.12), reached a peak at 3 h (1.63 ± 0.24), and returned to baseline (1.05 ± 0.15) after 12 h (Fig. 1B). These data indicate that LPS induced the phosphorylation of ezrin in a concentration- and time-dependent manner.

LPS activated the RhoA/ROCK signaling pathway in A549 cells

To investigate the potential involvement of the RhoA/ROCK signaling pathway in LPS-induced intracellular events, we examined the activity of GTP-RhoA (active form) using a RhoA activity assay. LPS upregulated the activity of GTP-RhoA in a time- dependent manner; peak activity occurred at 3 h (Fig. 2A). ROCK is a major downstream effector for Rho. The expression of ROCK1 was detected in the lungs, liver, kidneys, spleen, and testes, while ROCK2 was particularly expressed in the heart and brain. We also found that ROCK1 was also markedly up-regulated following LPS treatment (Fig. 2B) with a similar time course as GTP-bound RhoA.

ROCK mediates LPS-induced ezrin phosphorylation and relocation

The involvement of ROCK in LPS-induced ezrin activation was evaluated by using Y-27632, a preferential inhibitor of ROCK. The levels of P-ezrin increased significantly in LPS-treated cells; pre-treatment with Y-27632 markedly inhibited the upregulation of p-ezrin (Fig. 3A). Next, we investigated the intracellular

localization of ezrin by immunofluorescence. Resting cells exhibited weak green staining for p-ezrin that was mostly localized in the cytoplasm. Interestingly, p-ezrin appeared to translocate from the cytoplasm to the cell membrane in response to LPS, as evidenced by green punctuate staining; this was further indicated by co-localization with the reorganization of the F-actin cytoskeleton. This phenomenon was significantly abrogated by pre-treatment with Y-27632 (Fig. 3B).

Ezrin associated with MyD88/IRAK1 and Syk following LPS stimulation

Moesin has been identified as part of a protein cluster that is involved in cell signaling in response to LPS. The blockade of moesin interrupted the LPS-induced production of inflammatory cytokines *via* the inhibition of MyD88/IRAK1 [16]. Syk, a non-receptor protein tyrosine kinase, has been reported to associate with ezrin and facilitate the phosphorylation of ezrin [17]. Thus, we next evaluated potential interactions between ezrin and MyD88/IRAK1 or Syk. Following the immunoprecipitation of ezrin, western blotting of precipitated fractions showed that ezrin and Syk were present in both control and LPS-stimulated samples; however, the interaction between ezrin and MyD88/IRAK-1 only occurred in LPS-stimulated samples. These results indicate that ezrin interacts with Syk in a constitutive manner, but associates with MyD88/IRAK1 in an LPS stimulation-dependent manner (Fig. 4).

The suppression of ezrin inhibited the LPS-induced activation of p38 and NF-κB

To explore ezrin-mediated downstream signaling, A549 cells were treated with ezrin-siRNA and then exposed to LPS. The suppression of ezrin mRNA and protein expression was detected by qRT-PCR and western blotting. The transfection of ezrin-siRNA led to a marked reduction of ezrin levels (Fig. 5A, B). It has been shown that ERMs participates in the NF-κB and MAPKs signaling pathways [18–20]. Therefore, we investigated the potential involvement of p38, ERK1/2, JNK, IKK, IκBα, and NF-κB, in ezrin signaling. The phosphorylation of IKK, IκBα, p38, ERK, and JNK, as carried out by Western blotting, revealed a marked increase in LPS-treated A549 cells that were transfected with control siRNA (Fig. 5C). Similarly, the activation of NF-κB, as determined by EMSA, was increased in cells that were transfected with control siRNA and exposed to LPS (Fig. 5D). However, the suppression of ezrin partially suppressed LPS-induced NF-κB and p38 activation but not ERK1/2 and JNK phosphorylation, thus suggesting that ezrin lies upstream of the NF-κB and p38 signaling pathways under LPS condition (Fig. 5C, D).

The ROCK-ezrin pathway mediated the LPS-induced production of cytokines

To determine the functional relevance of ROCK-ezrin signaling in LPS-induced inflammatory responses, we next examined the effect of suppressing ROCK-ezrin activation on the production of pro-inflammatory cytokines in A549 cells. As expected, LPS induced a significant increase in the release of TNF-α, IL-1β,

and HMGB1 (Fig. 6A-C), and the cellular levels of HMGB1 (Fig. 6D). However, this up-regulation was inhibited by Y-27632 pre-treatment (Fig. 6A-D). CCK-8 assays showed that Y-27632 was not cytotoxic at the concentrations tested herein, thus suggesting that changes in the levels of HMGB1 were not due to passive release from necrotic cells (Fig. 6E).

It has previously been shown that ERM contributes to the LPS-induced production of cytokines [7, 8, 16]. As expected, LPS induced an increase in TNF-α, IL-1β, and HMGB1 in the cell culture supernatant (Fig. 6F-6H), and the cellular levels of HMGB1 (Fig. 6I). The suppression of ezrin dramatically inhibited LPS-induced increases in the production of TNF-α, IL-1β, and HMGB1 (Fig. 6F-6I).

Discussion

ALI and its severe form, ARDS, are potentially fatal complications of sepsis and important causes of high mortality in critically ill patients [21]. Several recent studies have linked ERM to LPS-induced lung injury [4–6]. However, the specific role of ezrin during this process has yet to be elucidated. In this paper, we describe a critical function for ezrin in LPS-induced pro-inflammatory cytokine production.

Our results demonstrate that LPS induced the phosphorylation of ezrin in a concentration- and time-dependent manner. LPS up-regulated RhoA activity and ROCK expression. The blockade of the RhoA/ROCK signaling pathway inhibited LPS- induced ezrin phosphorylation and its translocation from cytoplasm to cell membrane. Interestingly, ezrin interacted with Syk in a constitutive manner; in contrast, ezrin only associated with MyD88/IRAK1 under LPS challenge. Further analysis demonstrated that LPS-induced p38 and NF-κB activation was ezrin-dependent. More importantly, the suppression of ezrin by siRNA, or the blockade of ROCK activation with Y-27632, led to a reduction in the production of TNF-α, IL-1β and HMGB1 in response to LPS. These findings provide evidence that ezrin is upregulated in a RhoA/ROCK-dependent manner by LPS and that ezrin acts as an upstream regulator of p38 and NF-κB activation and the production of pro-inflammatory cytokines.

As a member of the ERM protein family, ezrin is considered not only as a cross-linker between the cytoskeleton and plasma membrane, but also an important signal transducer that participates in cell adhesion and motility [22]. For these cellular functions, ezrin needs to be activated. When subjected to stimuli, ezrin binds to phosphatidylinositol 4,5-bisphosphate (PIP2) in the cell membrane and subsequently the threonine residue (ezrin^{T567}) at the C-terminal is phosphorylated, thus leading to dissociation between the N-terminal and C-terminal domains; this unmasks binding sites for other molecules [23]. ERMs are phosphorylated by TNF-α, advanced glycation end products (AGEs), 2-Methoxyestradiol, and thrombin, and are known to modulate endothelial hyperpermeability [24–27]. Here, we report the phosphorylation of ezrin induced by LPS, as well as its translocation from the cytoplasm to the cell membrane in manner that is concomitant with the reorganization of the F-actin cytoskeleton. It has been shown that ERMs are translocated to the plasma membrane as a result of interactions with the cytoplasmic domain of integral membrane proteins, such as CD44, thus providing a site for association with actin filaments [28]. Thus, LPS-induced ezrin phosphorylation was accompanied by cytoskeleton

reorganization, indicating that LPS-induced conserved threonine residue phosphorylation might contribute to the formation of actin filaments and the reorganization of the actin cytoskeleton. These results are consistent with previous findings in pulmonary endothelial cells that were stimulated by TNF-α [24], 2-Methoxyestradiol [25], and thrombin [27], thus suggesting that the activation of ezrin is part of a general response to inflammatory stress [29].

Several protein kinases, including Rho/ROCK and PKC, are known to phosphorylate ERMs on the C-terminal threonine [30, 31]. ERMs can be directly phosphorylated by ROCK to enhance its binding to membrane proteins and F-actin, thus regulating the reorganization of actin filaments to participate in a range of cellular functions [32, 33]. In the present study, pre-treatment with Y-27632 prevented LPS-induced ezrin phosphorylation and its subsequent translocation from the cytosol to the cell membrane, as well as F-actin reorganization, thus suggesting a critical role for ROCK in the activation of ezrin. Interestingly, ERMs can play a dual role in the Rho/ROCK signaling pathway by acting both upstream and downstream of ROCK. ERMs can be activated by ROCK; once activated, ERMs dissociate Rho-GDI (a GDP dissociation inhibitor) from Rho and thereby activates Rho/ROCK [32, 33]. Thus, the rapid activation of ezrin and Rho/ROCK observed in the present study suggests that the levels of phosphorylated ezrin may act as a limiting factor for signaling pathways involving ezrin and that the marked upregulation of ezrin in response to LPS could be an important feed-forward mechanism.

Syk was originally identified in hemopoietic cells where it plays an important role in the regulation of the innate immune response [34]. Syk also acts as a key molecule in signaling processes that are initiated by pattern recognition receptors (PRRs); the role of this molecule in inflammation has been described in non-immune cells, such as the airway epithelium [35]. In a previous study, Urzainqui *et al.* showed that phosphorylation of the ITAM-like motif on ERMs is critical for recruiting Syk molecules, thus triggering cellular responses [36]. Zawawi *et al.* reported that cells stimulated with LPS showed clear phosphorylation of IRAK, although cells that were pre-incubated with an anti-moesin antibody exhibited total inhibition of IRAK phosphorylation and associations with IRAK MyD88 [16]. Therefore, it appears that ERMs act as an adapter protein that links Syk to MyD88/IRAK1. To decipher the likely associations between ezrin, Syk, and MyD88/IRAK1, in the presence of LPS, we next performed co-immunoprecipitation experiments. We found that the expression of Syk corresponded with that of ezrin, thus indicating that Syk interacts with ezrin in a constitutive manner. However, MyD88 and IRAK1 only immunoprecipitated with ezrin upon LPS challenge. These results demonstrate that ezrin interacts with MyD88/IRAK1 in a LPS stimulation-dependent manner and suggest that ezrin links Syk to MyD88/IRAK1 following LPS stimulation. ERMs play an important role in LPS- induced inflammation; however, the mechanisms involved remain unclear. Thus, our results suggest that the upregulation of ezrin, and its interaction with Syk/MyD88/IRAK1, can initiate Rho/ROCK-MyD88/IRAK1-ezrin/Syk signaling, and that this is one of the main mechanisms involved in the LPS.

To further explore the functional relevance of the ROCK-ezrin pathway in LPS- induced responses, we next used Y-27632 to inhibit ROCK activity and siRNA to suppress ezrin. We demonstrated that LPS induced significant reductions in the production of TNF-α, IL-1β, and HMGB1. The observed reduction in cytokine

production was associated with the inhibition of NF-κB and p38 MAPK activation. Interestingly, Zawawi *et al* [16] previously reported that the blockade of moesin function inhibited the LPS-induced activation of MyD88, IRAK and TRAF6, as well as subsequent MAPK activation and NF-κB translocation to the nucleus. Weng *et al*. [37] also confirmed that the phosphorylation of ezrin triggered MAPK signal transduction in tumor progression. Thus, our results are consistent with a specific role for the ERMs family in the activation of p38 and NF-κB activation.

Conclusions

Data presented in this manuscript provide novel insights into the molecular mechanisms and signaling pathways in the response of A549 cells to LPS. Based upon these findings, we suggest a model for LPS signaling events. In this model, LPS activates RhoA/ROCK and subsequently induces the phosphorylation of ezrin; this process requires the assistance of Syk. Phosphorylated ezrin then translocates from the cytoplasm to the plasma membrane where it recruits IRAK1 with the assistance of the MyD88 adaptor protein. The four-molecule cluster (ezrin, Syk, MyD88 and IRAK1) then induces activation of the NF-κB and p38 pathways and ultimately enhances the gene expression of inflammatory cytokines (Fig. 7).

Abbreviations

ALI
Acute lung injury
ANOVA
Analysis of variance
ARDS
Acute respiratory distress syndrome
BCA
Bicinchoninic acid
BSA
Bovine serum albumin
EMSAs
Electrophoretic mobility shift assays
ERMs
Ezrin/radixin/moesin proteins
HMGB1
High mobility group box 1 protein
IL-1β
Interleukin-1β
IRAK-1
IL-1R-associated kinase 1
LPS

Lipopolysaccharide
MAPK
Mitogen-activated protein kinase
MyD88
Myeloid differentiation factor 88
NF-κB
Nuclear factor-κB
PBS
Phosphate buffered saline
PIC
Protease inhibitor cocktail
PMSF
Phenylmethylsulfonyl fluoride
PVDF
Polyvinyl difluoride
RIPA
Radio immunoprecipitation assay
ROCK
Rho-associated coiled-coil containing protein kinase
SD
Standard deviation
SDS-PAGE
Sodium dodecyl sulfate polyacrylamide gel electrophoresis
TBST
Tris-buffered saline containing Tween 20
TLR4
Toll-like receptor 4
TNF-α
Tumor necrosis factor-α

Declarations

Ethical Approval and Consent to participate

Not applicable.

Consent for publication

Not applicable.

Availability of data and materials

All data generated in this study are available from corresponding author on reasonable request.

Competing interests

The authors declare that they have no competing interests.

Funding

This work was supported by grants from the National Natural Science Foundation of China (81772113), the Shandong Provincial Natural Science Foundation (ZR2020KF014), and the Science and Technology Planning Project of Guangdong (2016A020215017).

Authors' contributions

ND and HQL contributed to study design; HQL, BFG, YLL and ZZZ contributed to experimental studies; HQL, BFG, YLL and ZZZ contributed to data analysis; ND and HQL contributed to manuscript editing. All authors read and approved the final manuscript.

Acknowledgements

The authors would like to express their gratitude to EditSprings (https://www.editsprings.com/) for the expert linguistic services provided.

References

1. Matthay MA, et al. Acute respiratory distress syndrome. Nat Rev Dis Primers. 2019;5:18.
2. Domscheit H, et al. Molecular dynamics of lipopolysaccharide-induced lung Injury in rodents. Frontiers In physiology. 2020;11:36.
3. Kawaguchi K, et al. Pathophysiological roles of Ezrin/Radixin/Moesin proteins. Biol Pharm Bull. 2017;40,381 – 90.
4. Tang S, et al. Tumor necrosis factor-α requires Ezrin to regulate the cytoskeleton and cause pulmonary microvascular endothelial barrier damage. Microvasc Res. 2021;133:104093.
5. Fei L, et al. Phosphorylated ERM mediates lipopolysaccharide induced pulmonary microvascular endothelial cells permeability through negatively regulating Rac1 activity. Arch Bronconeumol. 2019;55,306 – 11.
6. Kovacs-Kasa A, et al. The protective role of MLCP-mediated ERM dephosphorylation in endotoxin-induced lung injury in vitro and in vivo. Sci rep. 2016;6:39018.
7. Pore D, et al. Cutting Edge: Ezrin regulates inflammation by limiting B cell IL-10 production. J Immunol. 2016;196,558 – 62.
8. Chen Y, et al. Moesin is a novel biomarker of endothelial injury in sepsis. J Immunol Res. 2021;2021,6695679.

9. Julian L, Olson MF. Rho-associated coiled-coil containing kinases (ROCK): structure, regulation, and functions. Small GTPases. 2014;5:e29846.
10. Fu C, et al. Activation of SIRT1 ameliorates LPS-induced lung injury in mice via decreasing endothelial tight junction permeability. Acta Pharmacol Sin. 2019;40,630 – 41.
11. Yang J, Ruan F, Zheng Z. Ripasudil attenuates lipopolysaccharide (LPS)-mediated apoptosis and inflammation in pulmonary microvascular endothelial cells via ROCK2/eNOS signaling. Med Sci Monit. 2018;24:3212–9.
12. Li Z, et al. Naringin attenuates MLC phosphorylation and NF-κB activation to protect sepsis-induced intestinal injury via RhoA/ROCK pathway. Biomed Pharmacother. 2018;103,50 – 8.
13. Liu Q, et al. Downregulation of p300 alleviates LPS-induced inflammatory injuries through regulation of RhoA/ROCK/NF-κB pathways in A549 cells. Biomed Pharmacother. 2018;97,369 – 74.
14. Wang Y, et al. Role of the Rho/ROCK signaling pathway in the protective effects of fasudil against acute lung injury in septic rats. Mol Med Rep. 2018;18:4486–98.
15. Kawano Y, et al. Phosphorylation of myosin-binding subunit (MBS) of myosin phosphatase by Rho-kinase in vivo. J Cell Biol. 1999;147:1023–38.
16. Zawawi KH, et al. Moesin-induced signaling in response to lipopolysaccharide in macrophages. J Periodontal Res. 2010;45:589–601.
17. Parameswaran N, et al. Spatial coupling of JNK activation to the B cell antigen receptor by tyrosine-phosphorylated ezrin. J Immunol. 2013;190:2017–26.
18. Ocaranza MP, et al. Rho-kinase pathway activation and apoptosis in circulating leucocytes in patients with heart failure with reduced ejection fraction. J Cell Mol Med. 2020;24:1413–27.
19. Fierro C, et al. Simultaneous Rho kinase inhibition in circulating leukocytes and in cardiovascular tissue in rats with high angiotensin converting enzyme levels. Int J Cardiol. 2016;215,309 – 17.
20. Zhu YW, et al. Knockdown of radixin suppresses gastric cancer metastasis in vitro by up-regulation of E-cadherin via NF-κB/Snail Pathway. Cell Physiol Biochem. 2016;39:2509–21.
21. Torres LK, et al. Attributable mortality of acute respiratory distress syndrome: a systematic review, meta-analysis and survival analysis using targeted minimum loss-based estimation. Thorax. 2021. doi:10.1136/thoraxjnl-2020-215950.
22. García-Ortiz A, Serrador JM. ERM proteins at the crossroad of leukocyte polarization, migration and intercellular adhesion. Int J Mol Sci. 2020;21:1502.
23. Braunger JA, et al. Phosphatidylinositol 4,5-bisphosphate alters the number of attachment sites between ezrin and actin filaments: a colloidal probe study. J Biol Chem. 2014;289:9833–43.
24. Zhou Q, et al. Inflammatory immune cytokine TNF-α modulates Ezrin protein activation via FAK/RhoA signaling pathway in PMVECs hyperpermeability. Front Pharmacol. 2021;12:676817.
25. Bogatcheva NV, et al. Ezrin, radixin, and moesin are phosphorylated in response to 2-methoxyestradiol and modulate endothelial hyperpermeability. Am J Respir Cell Mol Biol. 2011;45:1185–94.

26. Guo X, et al. ERM protein moesin is phosphorylated by advanced glycation end products and modulates endothelial permeability. Am J Physiol Heart Circ Physiol. 2009;297:H238–46.
27. Adyshev DM, et al. Ezrin/radixin/moesin proteins differentially regulate endothelial hyperpermeability after thrombin. Am J Physiol Lung Cell Mol Physiol. 2013;305:L240–55.
28. Fehon RG, McClatchey AI, Bretscher A. Organizing the cell cortex: The role of ERM proteins. Nat Rev Mol Cell Biol. 2010;11,276 – 87.
29. Michie KA, et al. Two sides of the coin: Ezrin/Radixin/Moesin and merlin control membrane structure and contact inhibition. Int J Mol Sci. 2019;20,1996.
30. Hébert M, et al. Rho-ROCK-dependent ezrin-radixin-moesinp hosphorylation cells regulates Fas-mediated apoptosis in Jurkat cells. J Immunol. 2008;181:5963–73.
31. Ng T, et al. Ezrin is a downstream effector of trafficking PKC-integrin complexes involved in the control of cell motility. EMBO J. 2001;20:2723–41.
32. Xiao Y, et al. Increased phosphorylation of ezrin is associated with the migration and invasion of fibroblast-like synoviocytes from patients with rheumatoid arthritis. Rheumatology (Oxford). 2014;53,1291 – 300.
33. Zarrin AA, et al. Kinase inhibition in autoimmunity and inflammation. Nat Rev Drug Discov. 2021;20:39–63.
34. Fu YL, Harrison RE. Microbial phagocytic receptors and their potential involvement in cytokine induction in macrophages. Front Immunol. 2021;12:662063.
35. Coates MS, et al. Pseudomonas aeruginosa induces p38MAP kinase-dependent IL-6 and CXCL8 release from bronchial epithelial cells via a Syk kinase pathway. PloS One. 2021;16:e0246050.
36. Urzainqui A, et al. ITAM-based interaction of ERM proteins with Syk mediates signaling by the leukocyte adhesion receptor PSGL-1. Immunity. 2002;17,401 – 12.
37. Weng W, et al. Phosphorylated T567 ezrin is associated with merlin expression in KIT-mutant gastrointestinal stromal tumors. Mol Med Rep. 2012;5:17–21.

Figures

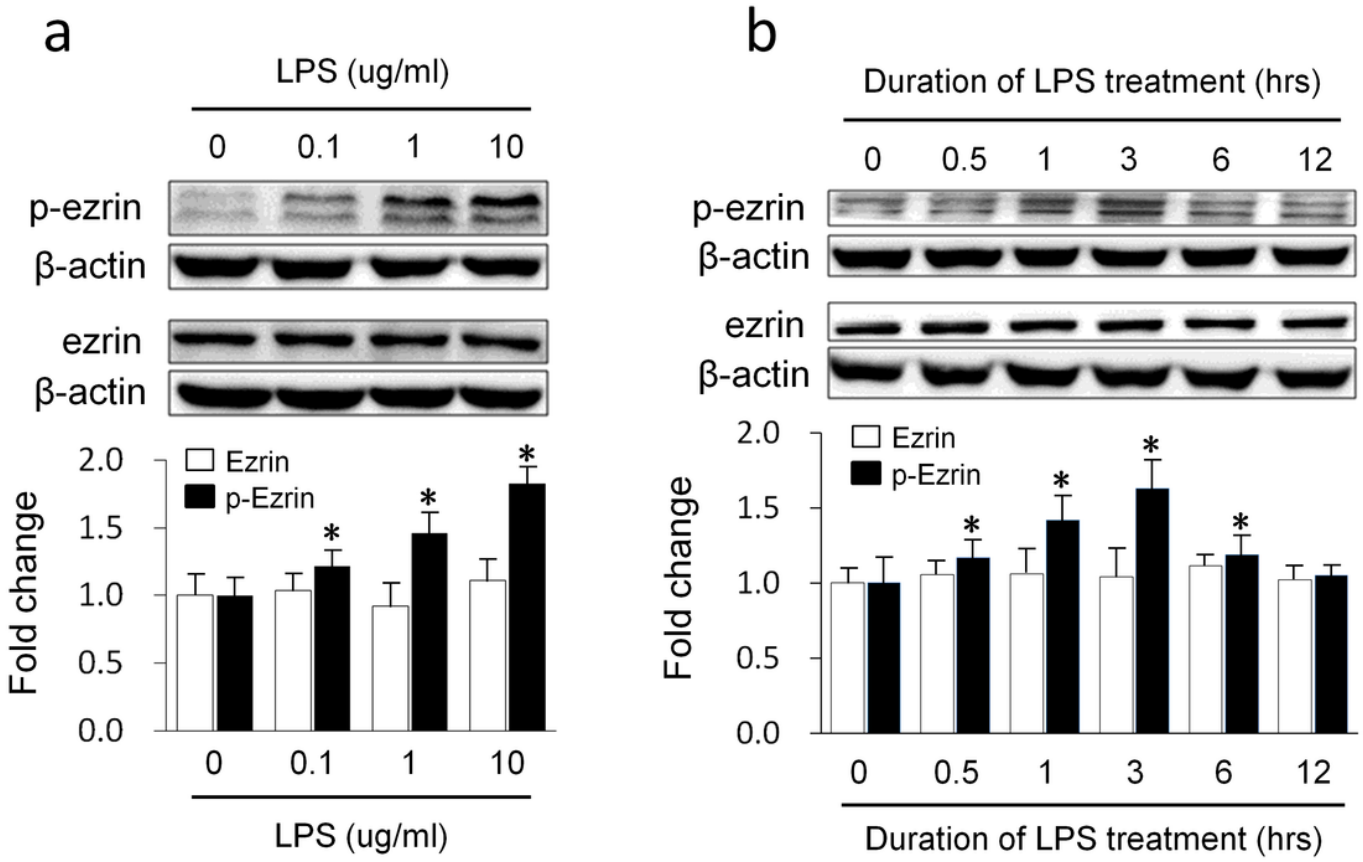

Figure 1

LPS induced ezrin phosphorylation in a concentration- and time- dependent manner. The effects of LPS on ezrin phosphorylation in A549 cells were analyzed by Western blotting. Total ezrin and p-ezrin were detected with a monoclonal antibody that recognized ezrin and polyclonal antibody recognizing phospho-ezrin (T567), respectively. β-actin was used as internal reference. (A) cells were treated with LPS for 3 h at concentrations of 0, 0.1, 1, and 10 μg/ml, respectively. (B) Cells were treated with LPS (10 μg/ml) for 0, 0.5, 1, 3, 6 and 12 h, respectively. Dates are expressed as means ±S D of triplicate samples. * $p < 0.05$ vs. 0 group.

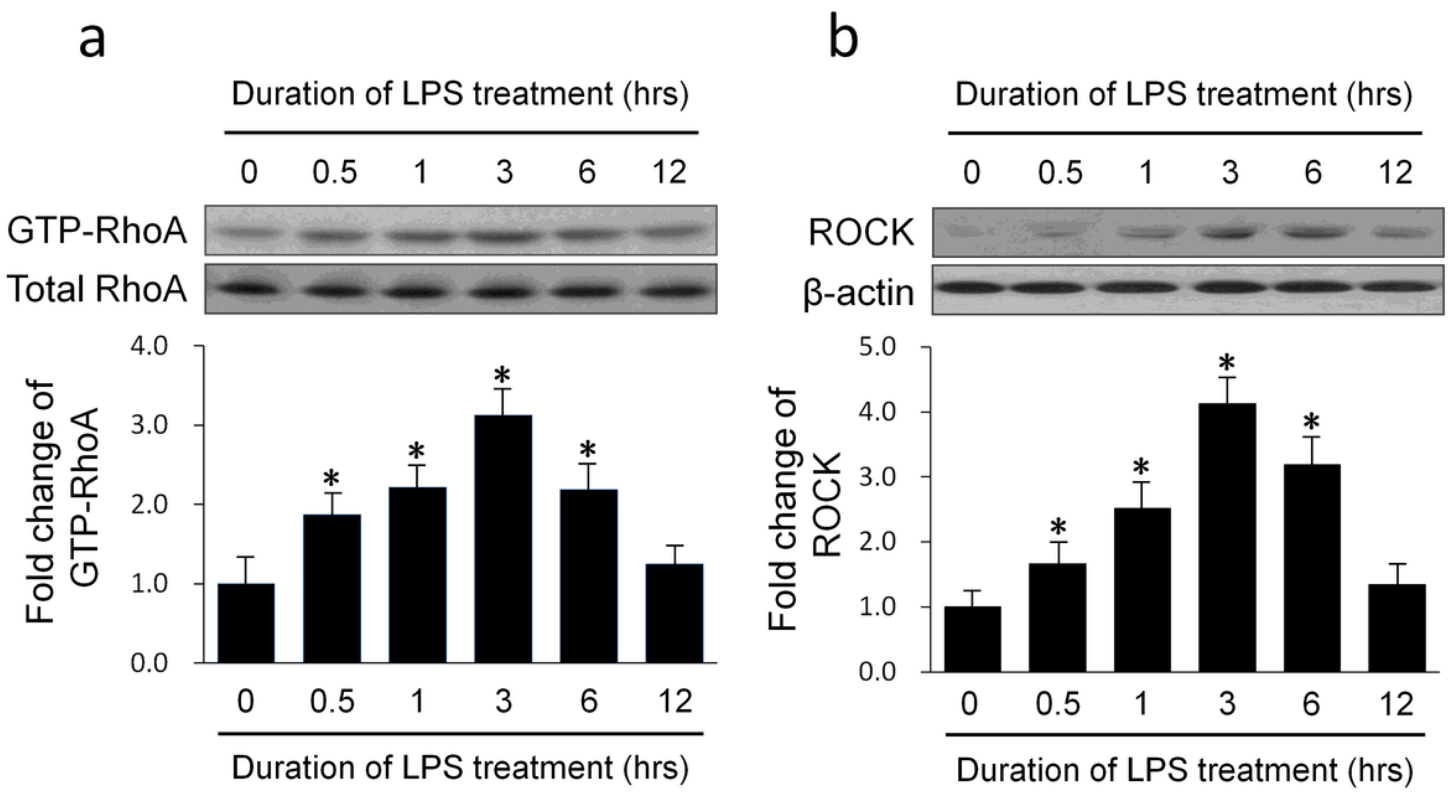

Figure 2

LPS up-regulated RhoA activity and ROCK expression in A549 cells. A549 cells were treated with 10 μg/ml of LPS for 0, 0.5, 1, 3, 6 and 12 h, respectively. (A) Effect of LPS on RhoA activity was assessed by RhoA activation assays. (B) The effects of LPS on ROCK expression were examined by Western blotting. β-actin was used as internal reference. Dates are expressed as means ± SD of triplicate samples. * $p<0.05$ vs. 0 group.

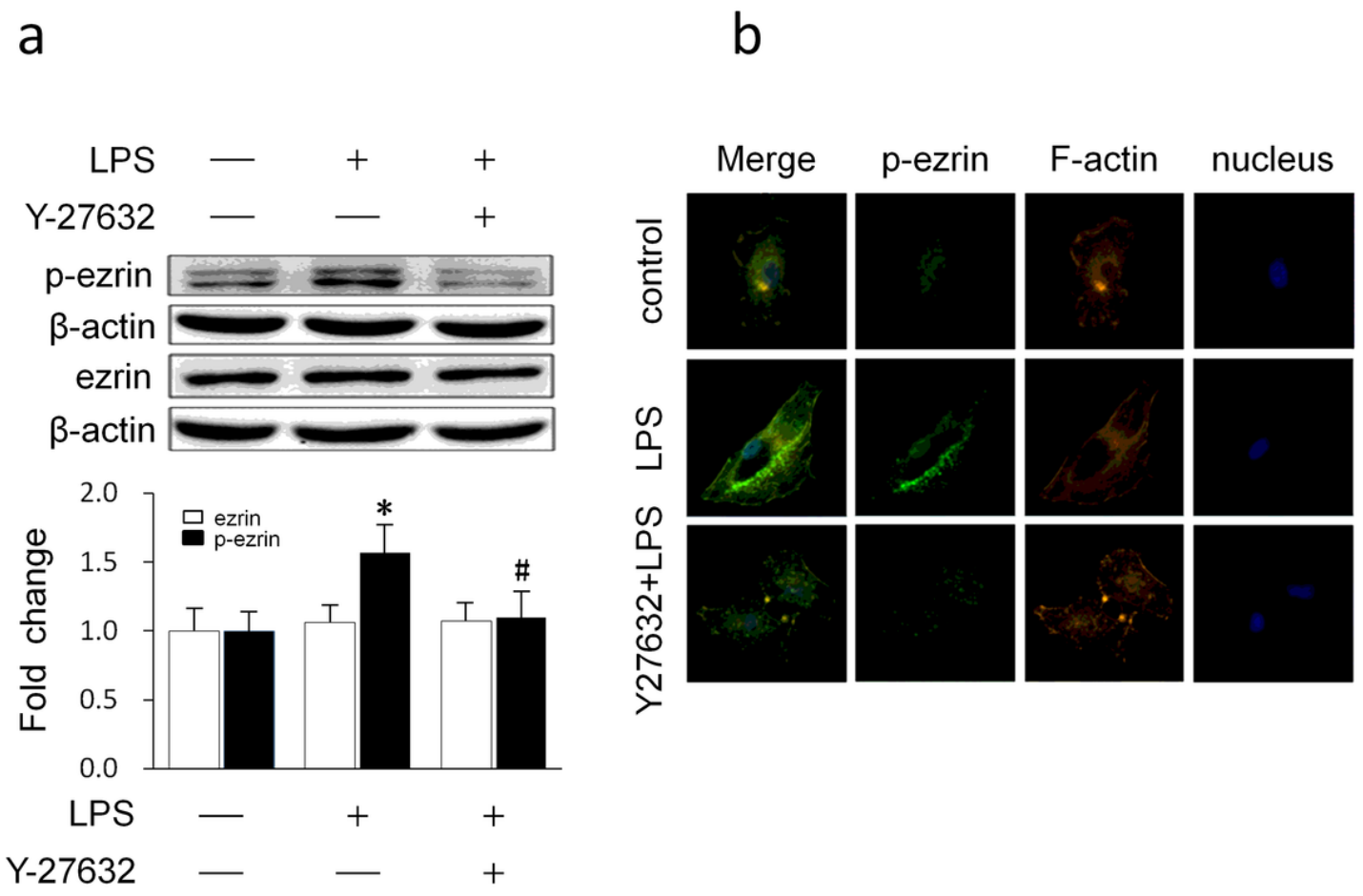

Figure 3

ROCK mediated LPS-induced ezrin phosphorylation and translocation For the LPS group, A549 cells were treated with 10 μg/ml of LPS for 3 h. For the Y-27632+LPS group, A549 cells were pre-treated with 50 μM of Y-27632 1 h prior to LPS treatment. (A) Total ezrin and p-ezrin protein levels were detected by western blotting using β-actin as an internal reference. Data are expressed as means ± SD of triplicate samples. *p<0.05 vs. control, #p<0.05 vs. LPS. (B) The intracellular localization of p-ezrin in resting and LPS-activated A549 cells was investigated by immunofluorescence. P-ezrin was stained with Alexa Fluor ®488-conjugated IgG (green), F-actin was stained with Rhodamine-phalloidin (yellow), and nuclei were stained with DAPI (blue). Qualitative analysis was performed by confocal microscopy (×60).

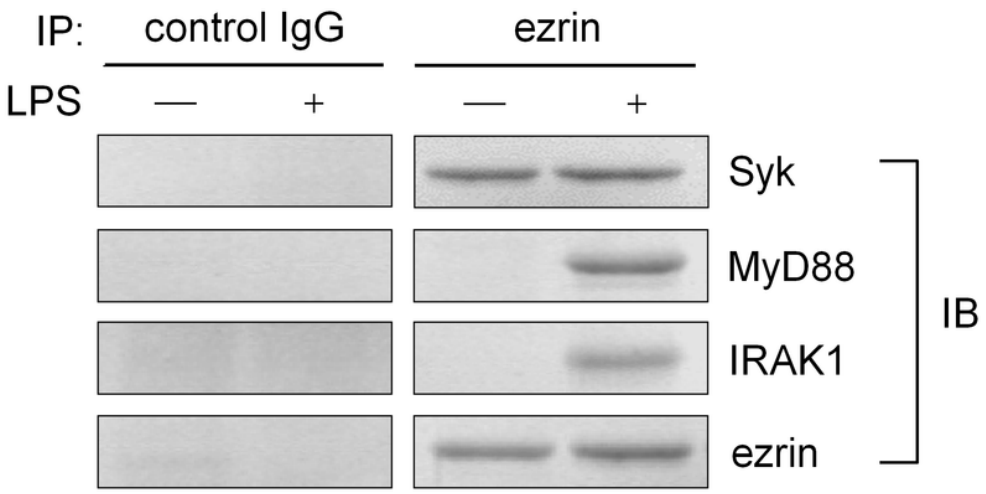

Figure 4

The association between ezrin, MyD88/IRAK1, and Syk Lysates isolated from A549 cells exposed to LPS (+) or without LPS (-) were immunoprecipitated in the presence of anti-ezrin or control IgG antibody, followed by western blotting with anti-Syk, anti-MyD88, or anti-IRAK1 antibodies. IP: immunoprecipitation, IB: immunoblotting.

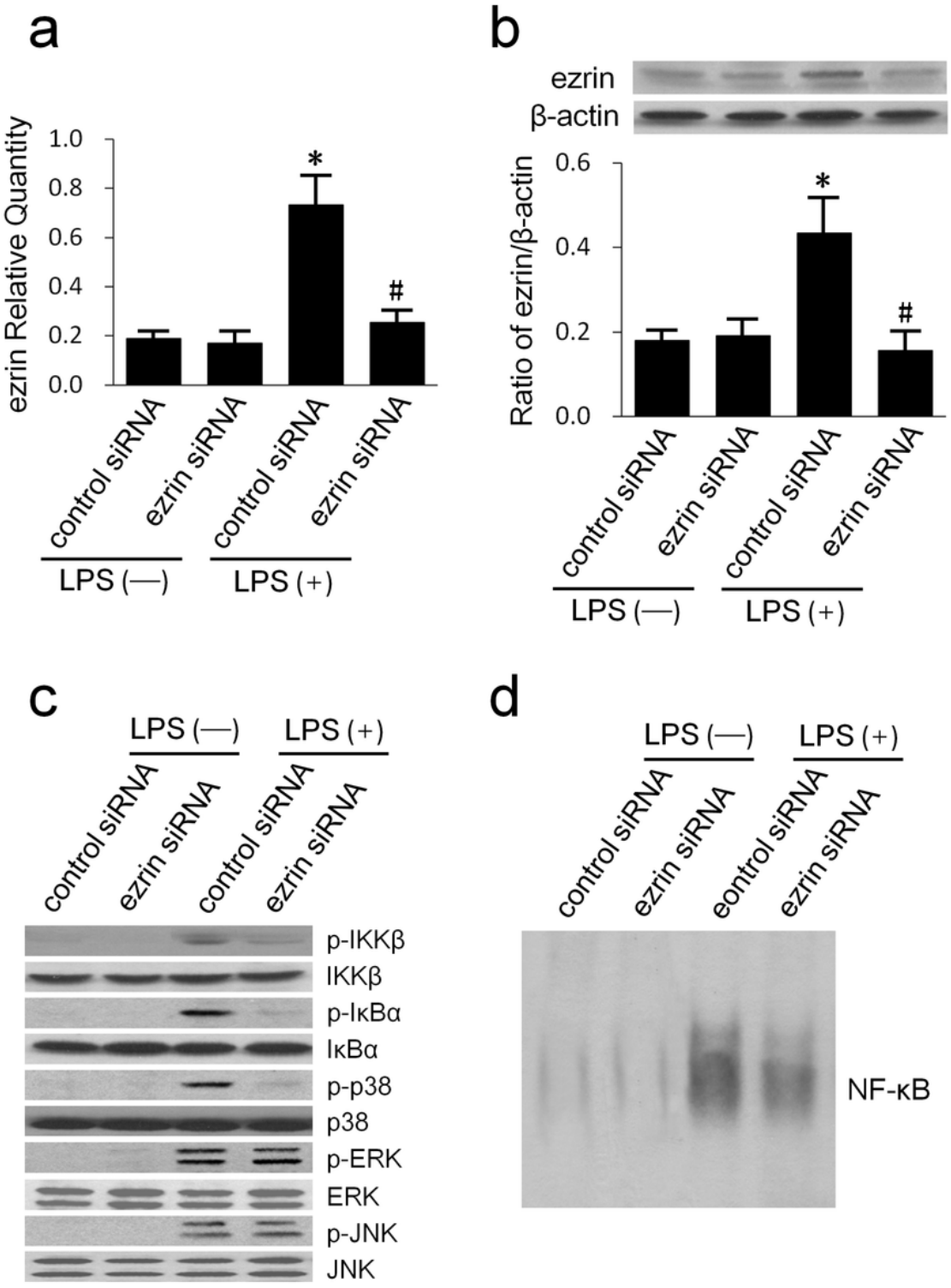

Figure 5

The suppression of ezrin inhibited the LPS-induced activation of p38 and NF-κB A549 cells were first transfected with ezrin-specific siRNA or control siRNA. Next, we detected the expression of ezrin mRNA and protein by qRT-PCR (A) and western blotting (B). The effect of ezrin siRNA transfection on IKK, IκBα, and MAPKs activation was detected by western blotting (C) and NF-κB activation, as determined by

EMSA (D). Data are expressed as mean ± SD of triplicate samples. *p<0.05 vs. LPS(-) group, #p< 0.05 vs. control siRNA group.

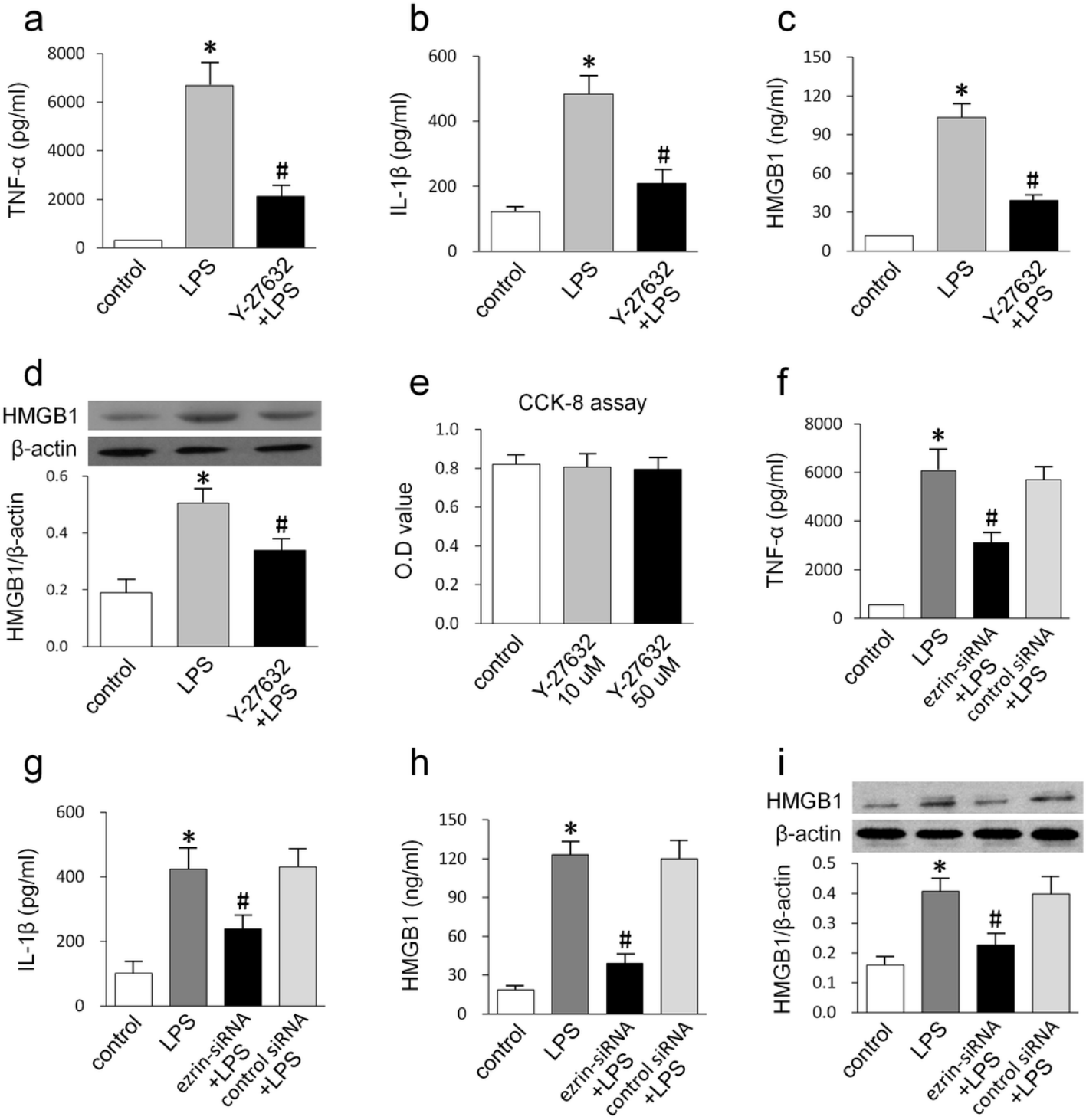

Figure 6

The suppression of ezrin inhibited the LPS-induced production of cytokines A549 cells were pre-treated with Y-27632 and subjected to LPS. The release of TNF-α, IL-1β, and HMGB1 into the supernatants were then measured by ELISA (A, B, C). The expression levels of HMGB1 in cell lysates were measured by western blotting (D). Cell viability was examined by CCK-8 assay (E). A549 cells were transfected with

ezrin-specific siRNA; TNF-α, and IL-1β expression was measured by ELISA (F, G, H) while HMGB1 release was measured by Western blotting (I). Data are expressed as mean ± SD of triplicate samples. *p<0.05 vs. control group, #p<0.05 vs. LPS group.

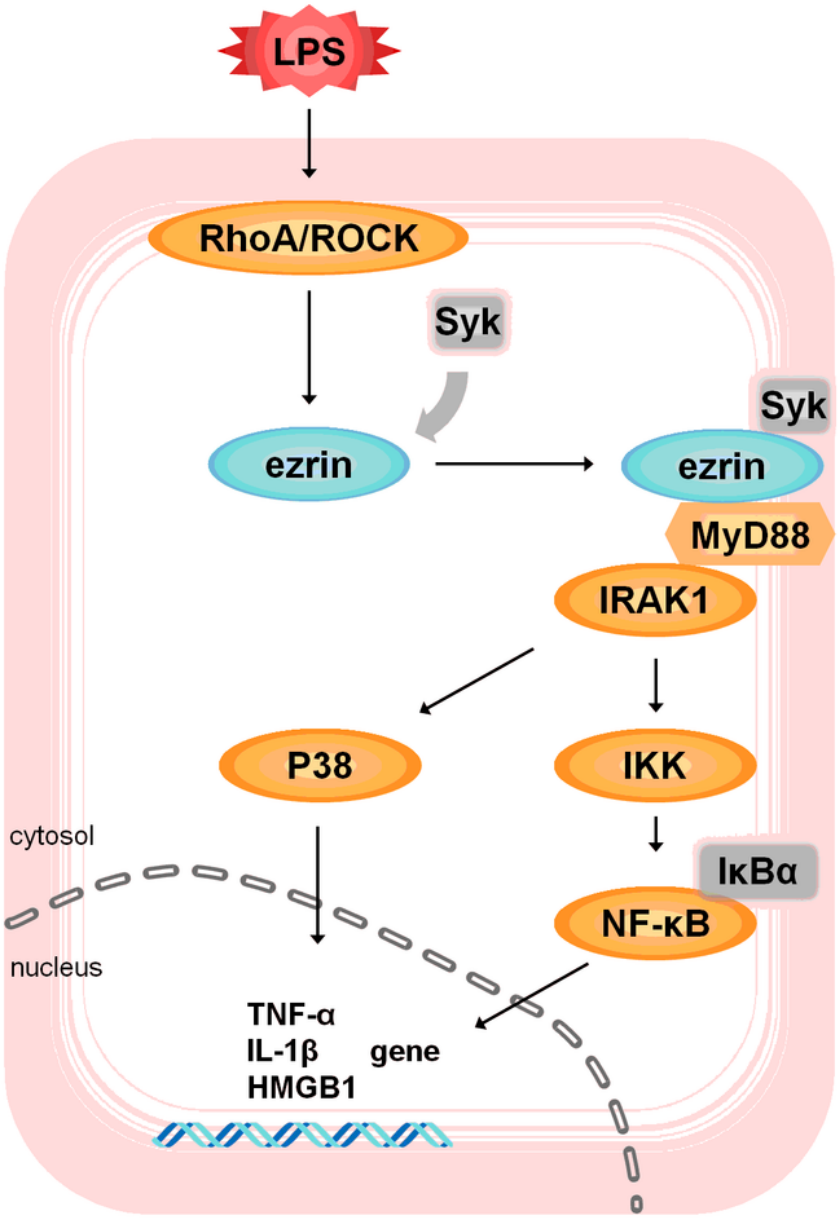

Figure 7

A schematic summary of the ROCK-ezrin pathway in response to LPS in A549 cells.